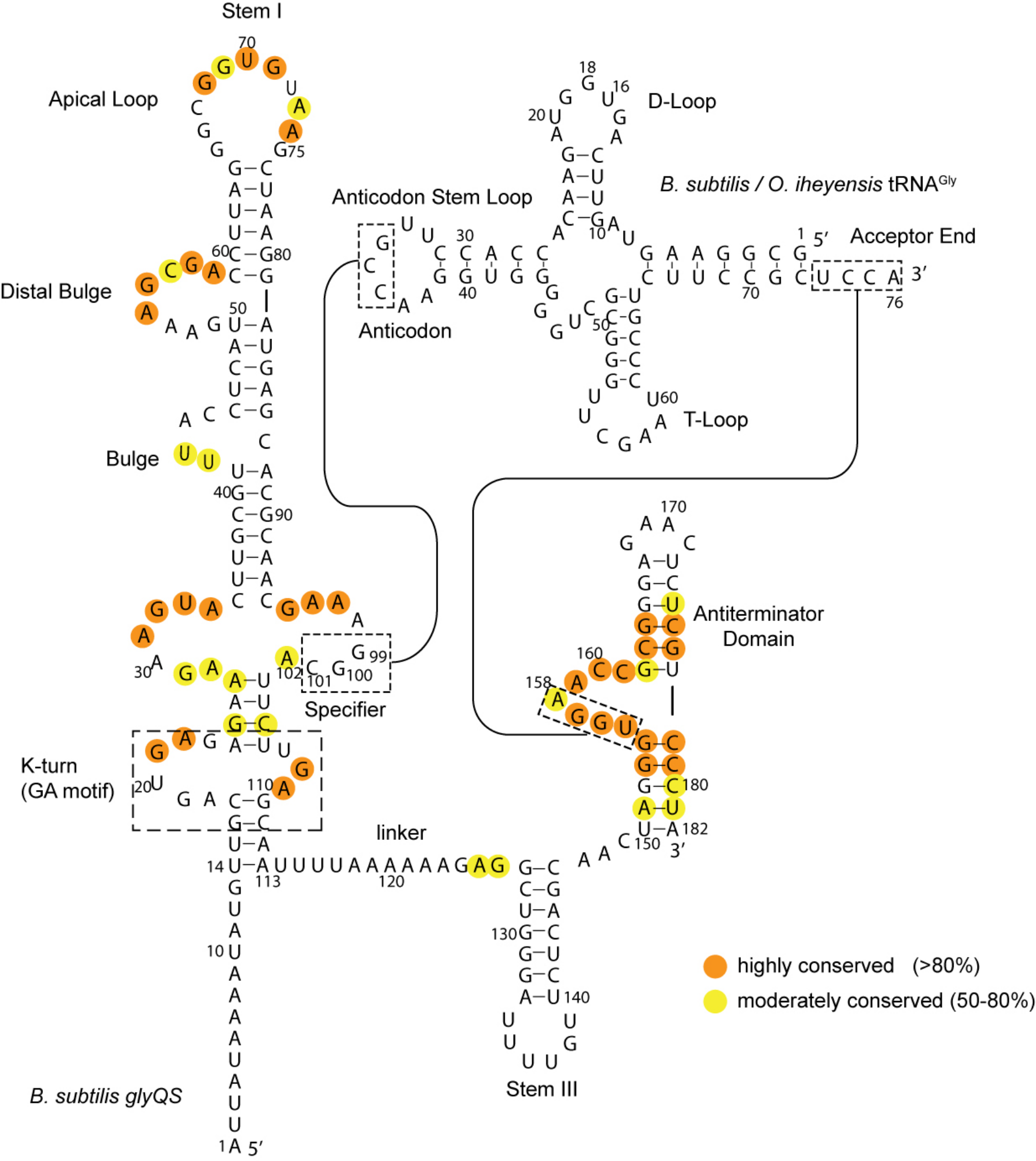
Stem I
Apical Loop
Distal Bulge
Bulge
K-turn
(GA motif)
Specifier
Anticodon Stem Loop
Anticodon
D-Loop
T-Loop
B. subtilis / O. iheyensis tRNAGly
Acceptor End
5′
3′
Antiterminator
Domain
linker
Stem III
B. subtilis glyQS
highly conserved (>80%)
moderately conserved (50-80%)

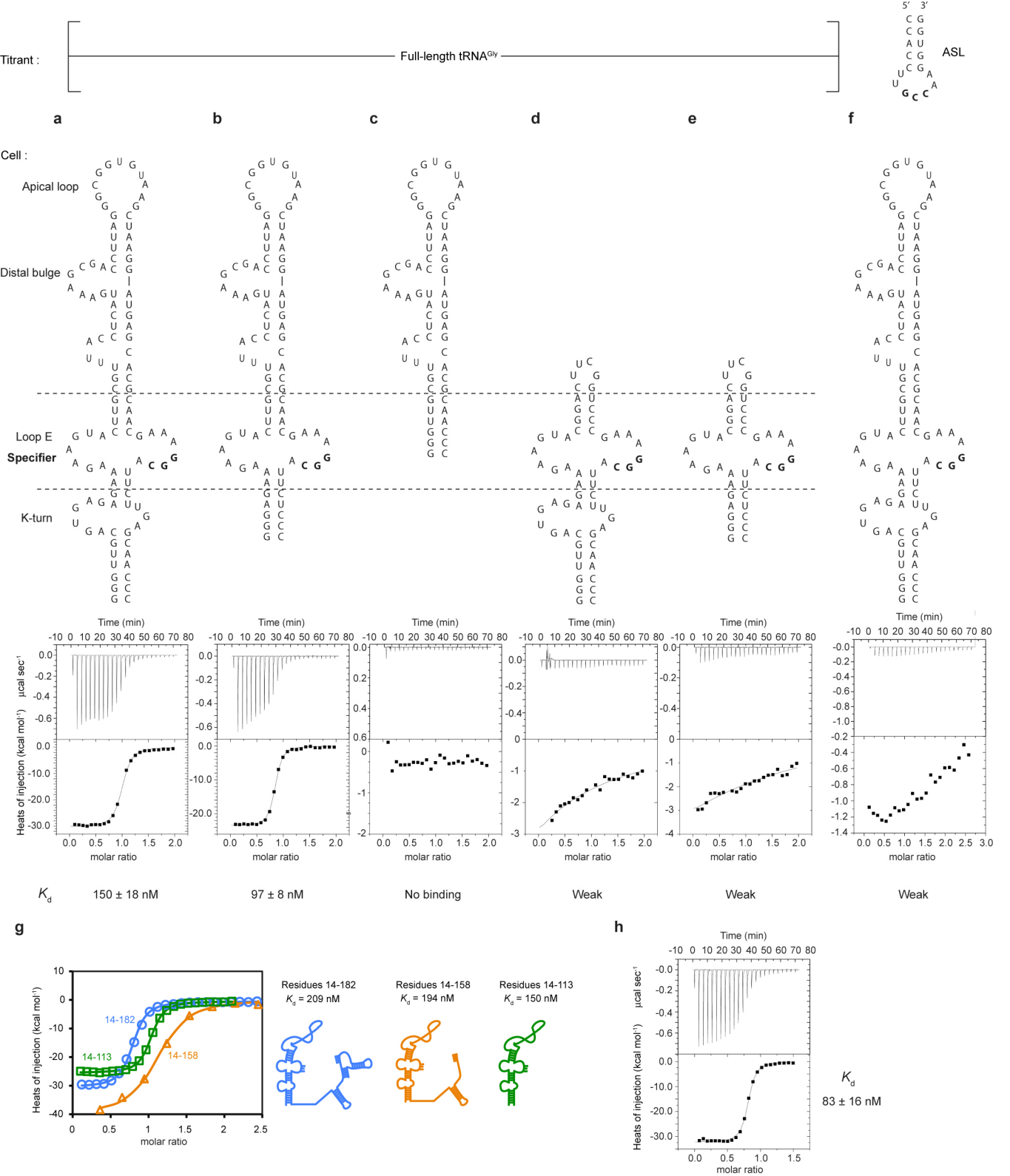
Titrant :
Full-length tRNA^Gly
ASL
a
b
c
d
e
f
Cell :
Apical loop
Distal bulge
Loop E
Specifier
K-turn
Time (min)
µcal sec⁻¹
Heats of injection (kcal mol⁻¹)
molar ratio
K_d
150 ± 18 nM
97 ± 8 nM
No binding
Weak
Weak
Weak
g
Heats of injection (kcal mol⁻¹)
molar ratio
14-182
14-158
14-113
Residues 14-182
K_d = 209 nM
Residues 14-158
K_d = 194 nM
Residues 14-113
K_d = 150 nM
h
Time (min)
µcal sec⁻¹
Heats of injection (kcal mol⁻¹)
molar ratio
K_d
83 ± 16 nM

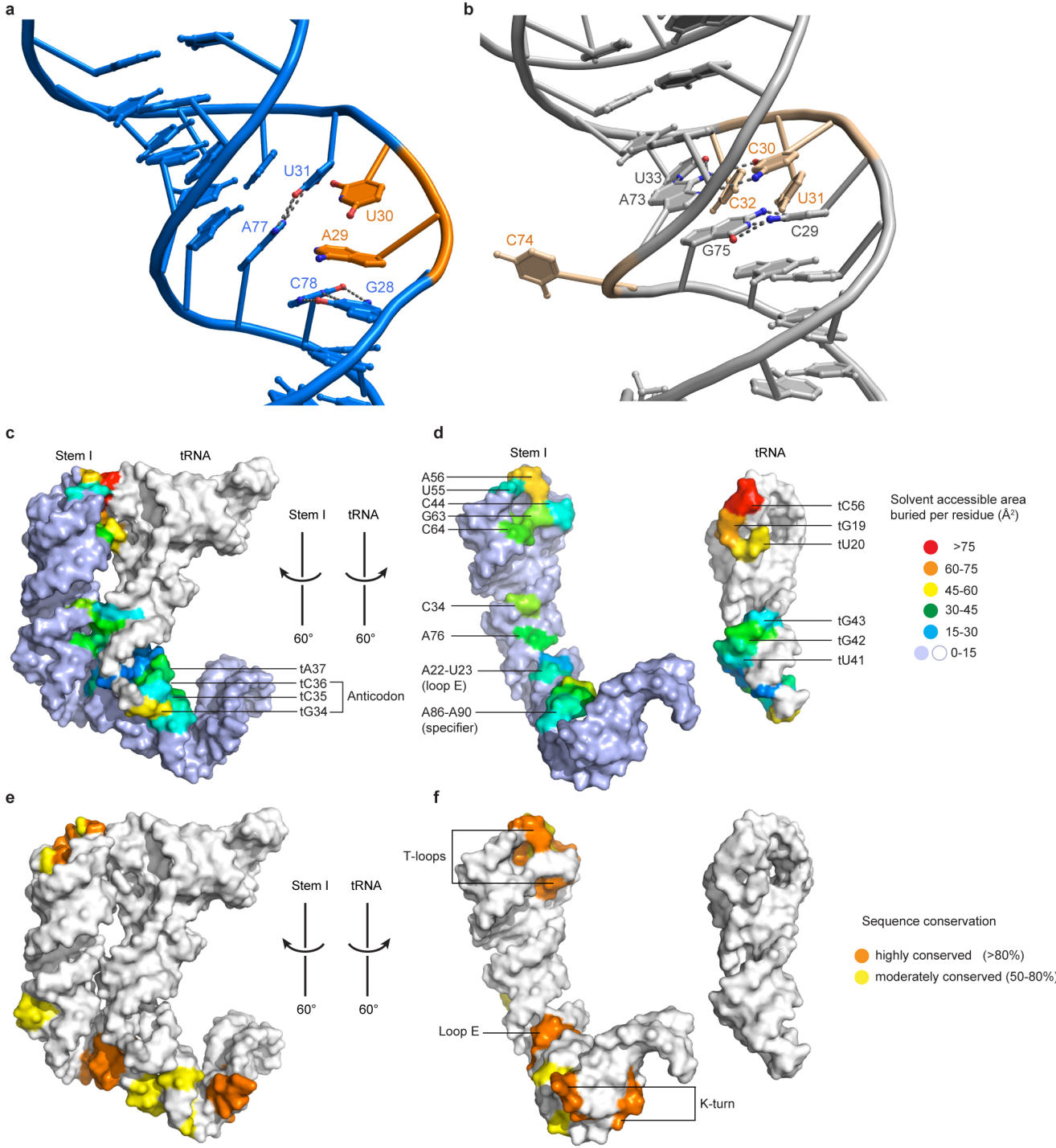
a
U31
A77
U30
A29
C78
G28
b
C30
U33
A73
C32
U31
C29
G75
C74
c
Stem I
tRNA
Stem I
tRNA
60°
60°
tA37
tC36
tC35
tG34
Anticodon
d
Stem I
tRNA
A56
U55
C44
G63
C64
C34
A76
A22-U23
(loop E)
A86-A90
(specifier)
tC56
tG19
tU20
tG43
tG42
tU41
Solvent accessible area
buried per residue (Å²)
>75
60-75
45-60
30-45
15-30
0-15
e
Stem I
tRNA
60°
60°
f
T-loops
Loop E
K-turn
Sequence conservation
highly conserved (>80%)
moderately conserved (50-80%)

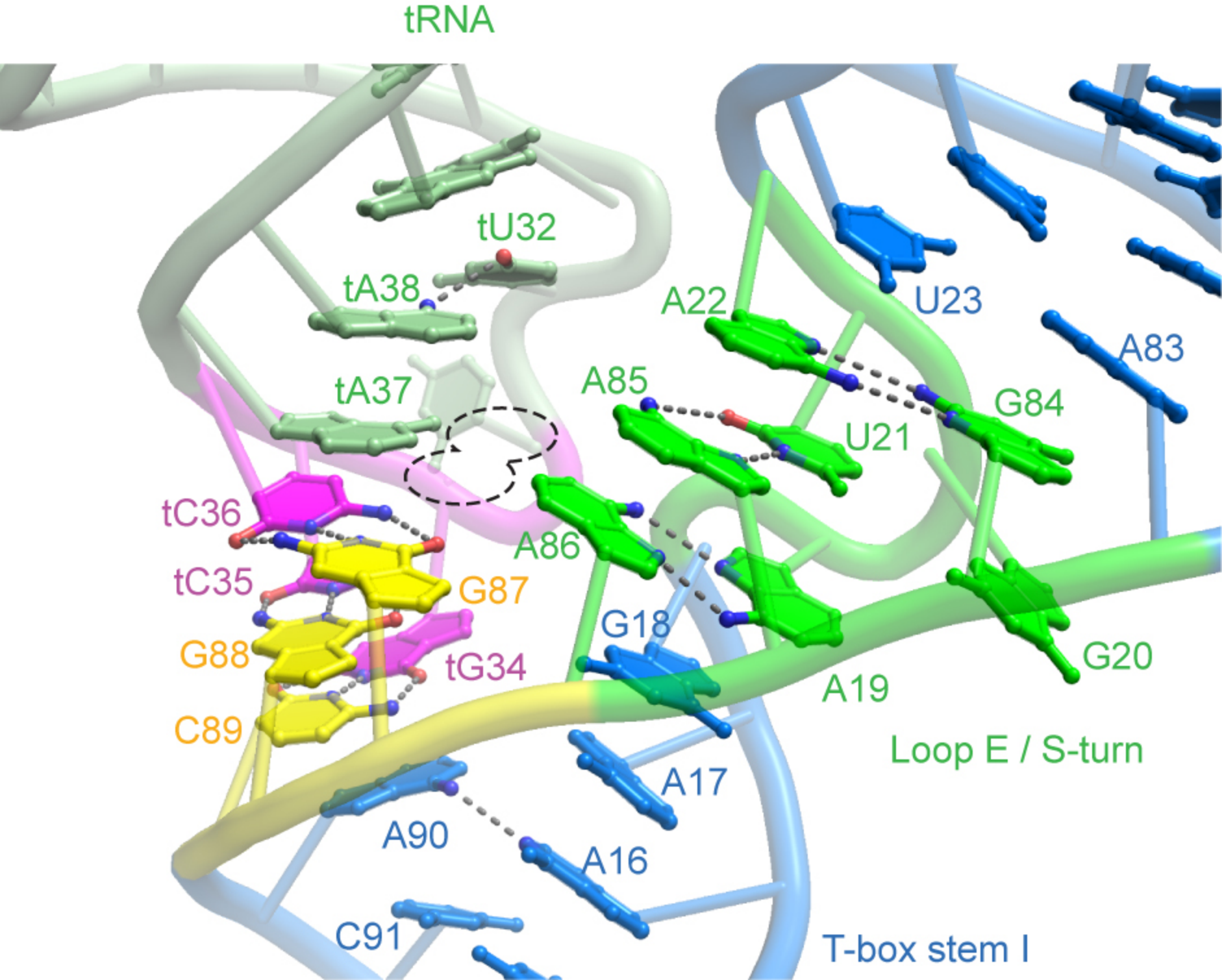
tRNA
tU32
tA38
tA37
tC36
tC35
G88
C89
G87
tG34
A86
A85
A22
U23
A83
G84
U21
G18
A19
G20
A17
A90
A16
C91
Loop E / S-turn
T-box stem I

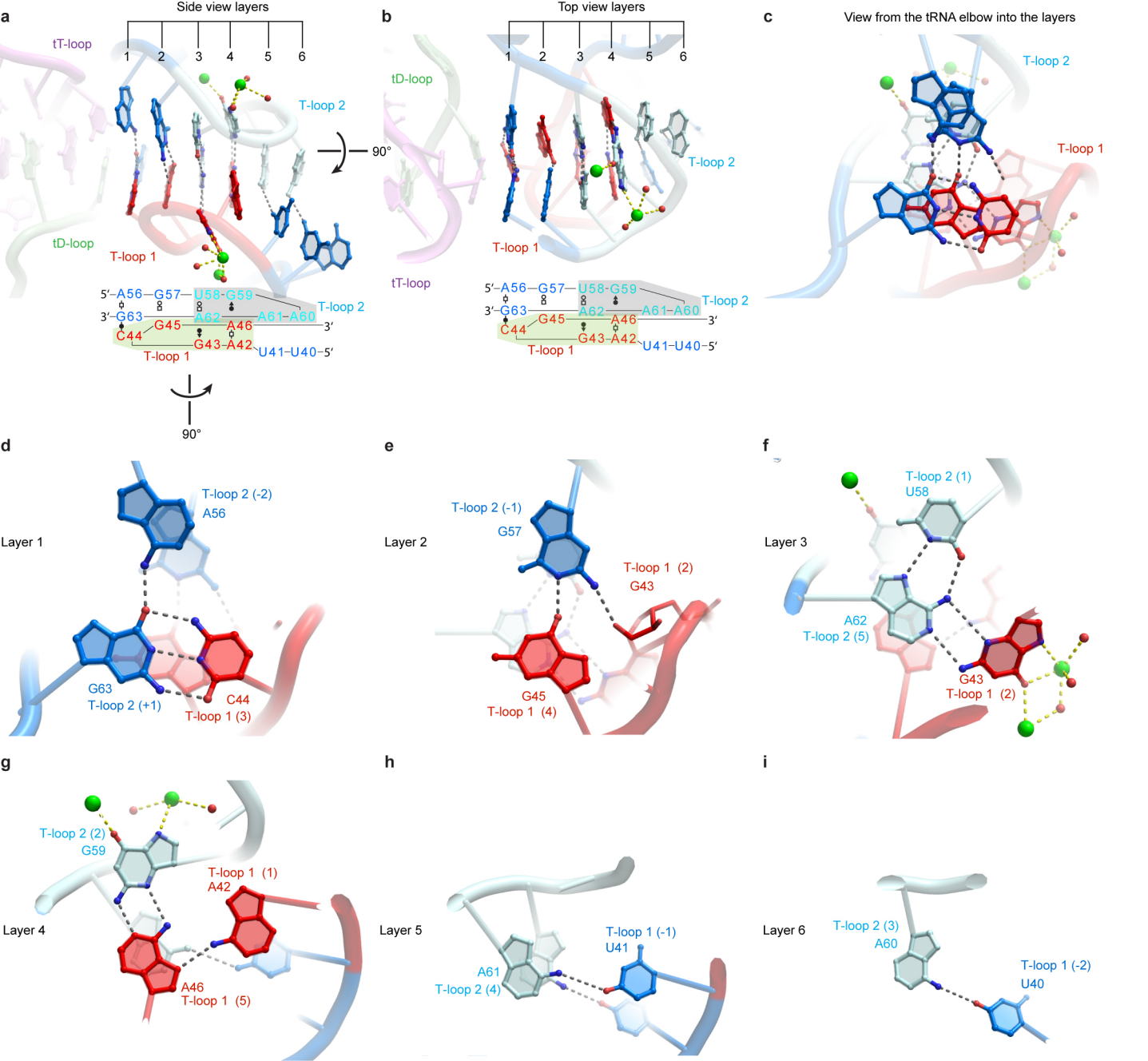
a
Side view layers
1
2
3
4
5
6
tT-loop
T-loop 2
90°
tD-loop
T-loop 1
5′–A56–G57–U58-G59
3′–G63–A62–A61–A60
C44–G45–A46
G43–A42–U41–U40–5′
T-loop 2
3′
T-loop 1
90°
b
Top view layers
tD-loop
T-loop 2
T-loop 1
tT-loop
c
View from the tRNA elbow into the layers
T-loop 2
T-loop 1
d
Layer 1
T-loop 2 (-2)
A56
G63
T-loop 2 (+1)
C44
T-loop 1 (3)
e
Layer 2
T-loop 2 (-1)
G57
T-loop 1 (2)
G43
G45
T-loop 1 (4)
f
Layer 3
T-loop 2 (1)
U58
A62
T-loop 2 (5)
G43
T-loop 1 (2)
g
Layer 4
T-loop 2 (2)
G59
T-loop 1 (1)
A42
A46
T-loop 1 (5)
h
Layer 5
T-loop 1 (-1)
U41
A61
T-loop 2 (4)
i
Layer 6
T-loop 2 (3)
A60
T-loop 1 (-2)
U40

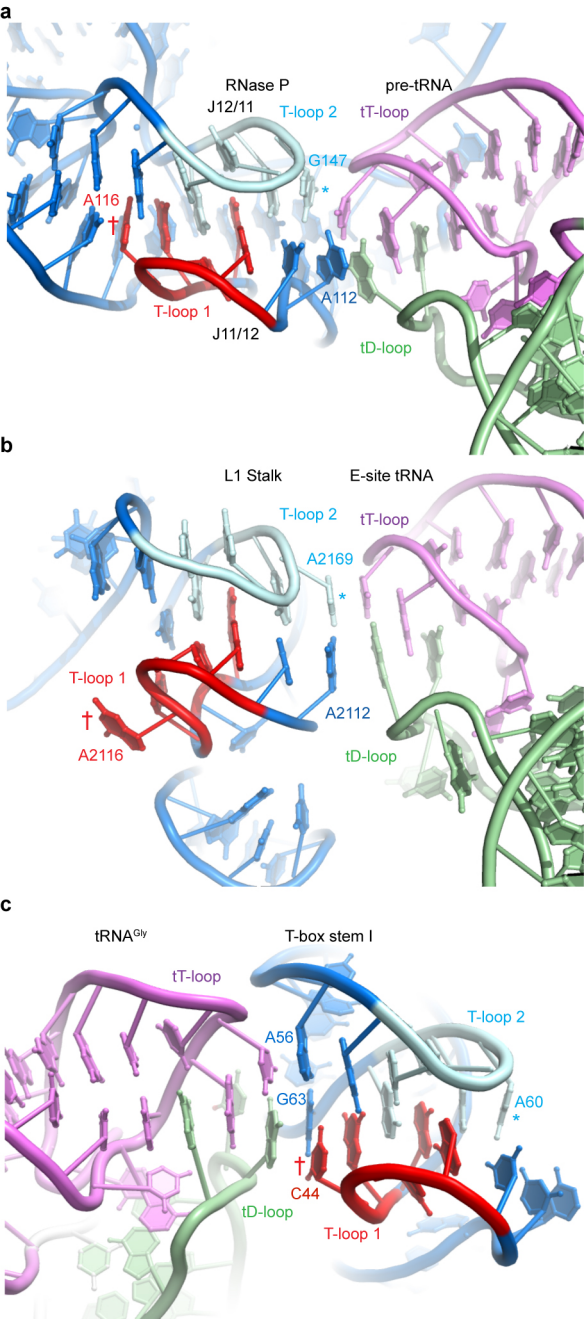
a
RNase P
pre-tRNA
J12/11
T-loop 2
tT-loop
G147
*
A116
†
T-loop 1
A112
J11/12
tD-loop
b
L1 Stalk
E-site tRNA
T-loop 2
tT-loop
A2169
*
T-loop 1
†
A2116
A2112
tD-loop
c
tRNAGly
T-box stem I
tT-loop
T-loop 2
A56
G63
A60
*
†
C44
tD-loop
T-loop 1

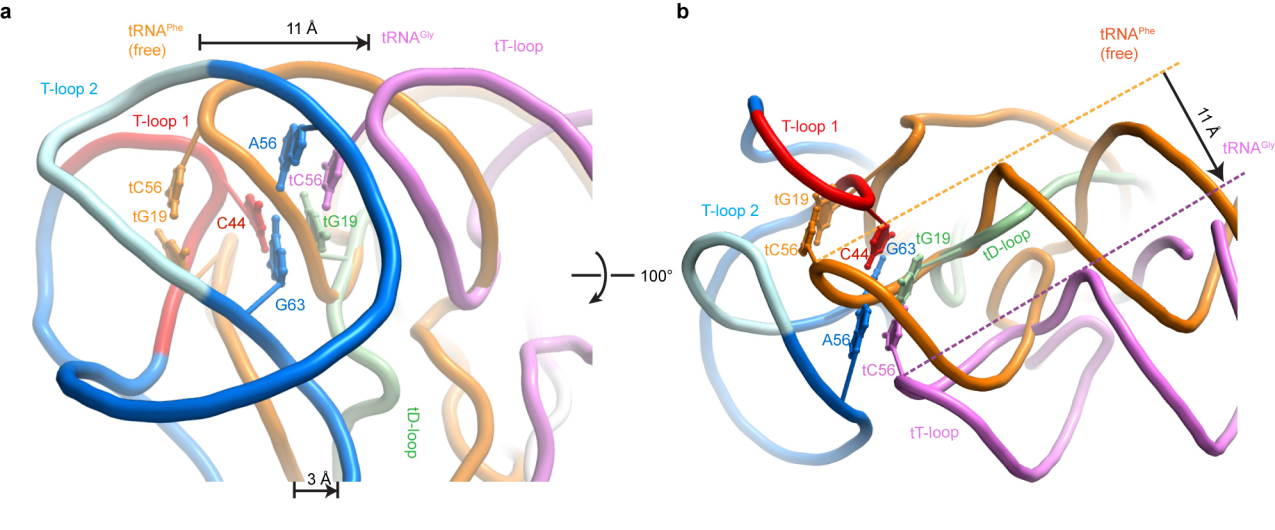
a
tRNAPhe
(free)
11 Å
tRNAGly
tT-loop
T-loop 2
T-loop 1
A56
tC56
tC56
tG19
C44
tG19
G63
tD-loop
3 Å
100°
b
tRNAPhe
(free)
11 Å
tRNAGly
T-loop 1
tG19
T-loop 2
tC56
C44
G63
tG19
tD-loop
A56
tC56
tT-loop

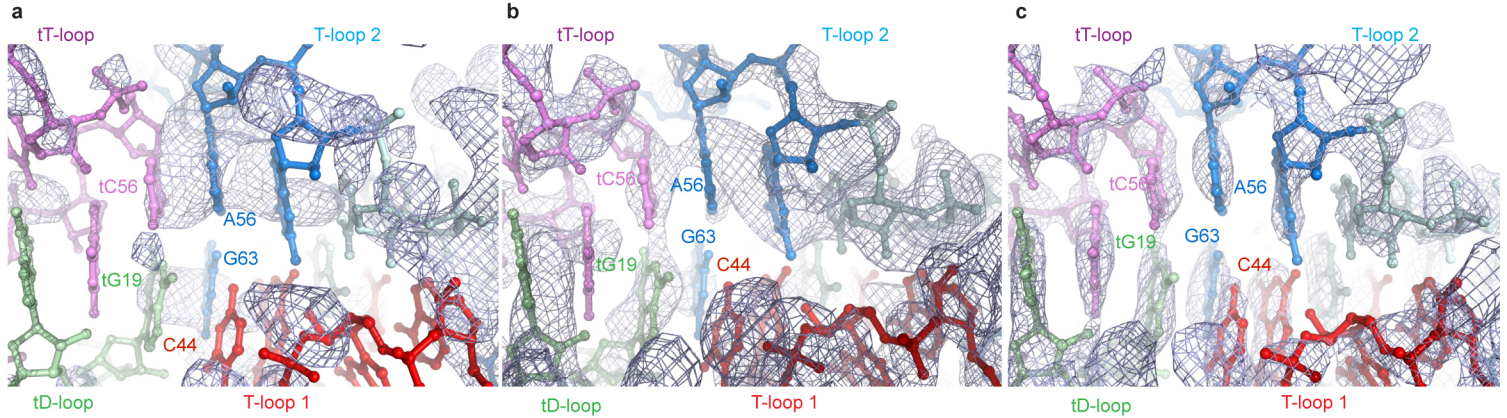
a
tT-loop
T-loop 2
tC56
A56
G63
tG19
C44
tD-loop
T-loop 1
b
tT-loop
T-loop 2
tC56
A56
G63
tG19
C44
tD-loop
T-loop 1
c
tT-loop
T-loop 2
tC56
A56
G63
tG19
C44
tD-loop
T-loop 1

T-box *	$tRNA^{Gly}$	K_d (μM)	log[K_a]	ΔH (kcal mol^{-1})	$-T\Delta S$ (kcal mol^{-1}) †
14-182 (wt) ‡	wt	0.209 ± 0.025	6.68	-29.9	21.0
14-158 (wt) §	wt	0.194 ± 0.055	6.72	-41.2	32.2
14-113 (wt) ||	wt	0.150 ± 0.018	6.82	-25.1	15.9
14-113del_kturn ¶	wt	0.097 ± 0.008	7.01	-23.6	14.2
Δ29-30 (Δ42-43)	wt	1.84 ± 0.42	5.74	-27.0	19.3
G43U (G55U)	wt	1.68 ± 0.16	5.78	-39.7	31.9
C44U (C56U)	wt	8.20 ± 2.9	5.08	-45.3	38.5
C44A (C56A)	wt	0.307 ± 0.038	6.51	-30.7	21.9
C44G (C56G)	wt	3.4 ± 2.3	5.47	-42.1	34.7
A42G/A46G (A54G/A58G)	wt	9.0 ± 2.1	5.05	-30.0	23.2
G56U (G68U)	wt	4.6 ± 0.44	5.34	-32.0	24.8
G56A (G68A)	wt	0.406 ± 0.060	6.39	-33.2	24.6
G59U (G71U)	wt	0.538 ± 0.12	6.27	-45.4	36.9
G59A (G71A)	wt	1.69 ± 0.30	5.77	-43.0	35.2
A61U (A73U)	wt	0.125 ± 0.019	6.90	-35.4	26.1
U58G/A62G (U70G/A74G)	wt	12.6 ± 8.3	4.90	-28.2	21.6
G63C (G75C)	wt	8.7 ± 0.84	5.06	-30.0	23.2
C44G/G63C (C56G/G75C)	wt	1.9 ± 1.5	5.72	-39.8	32.2
C44A/G63A (C56A/G75A)	wt	0.433 ± 0.31	6.36	-32.0	23.5
G87U (G99U)	tC36A	7.6 ± 4.2	5.12	-17.2	10.4
A90C (A102C)	wt	0.641 ± 0.167	6.19	-26.9	18.6
A90G (A102G)	wt	0.070 ± 0.012	7.15	-31.5	21.9
14-113 (wt)	tA37U	0.125 ± 0.018	6.90	-35.4	26.1
14-113 (wt)	3'GAAA #	0.083 ± 0.016	7.08	-31.8	22.3

	Crystal I	Crystal II	Crystal III	Crystals I-II-III
Data collection				
Space group	$C222_1$	$C222_1$	$C222_1$	$C222_1$
Cell dimensions				
a, *b*, *c* (Å)	100.3, 108.4, 266.8	99.1, 107.5, 266.1	100.3 ,108.3, 267.8	100.0, 108.1, 266.9
α, β, γ (°)	90, 90, 90	90, 90, 90	90, 90, 90	90, 90, 90
Resolution (Å)	28.42-3.20 (3.31-3.20)*	133.1-3.87 (4.08-3.87)	133.9-3.76 (3.97-3.76)	134-3.43 (3.61-3.43)
R_{merge} (%)	6.2 (104.8)	6.2 (67.1)	6.7 (59.5)	10.8 (82.8)
$\langle I \rangle / \langle \sigma(I) \rangle$	11.1 (1.5)	14.3 (2.2)	14.2 (2.3)	23.7 (2.3)
Completeness (%)	98.9 (98.8)	99.8 (99.7)	99.4 (99.2)	99.3 (96.0)
Redundancy	6.1 (6.2)	4.8 (4.8)	4.8 (4.7)	12.8 (6.2)
Refinement				
Resolution (Å)	28.42-3.20 (3.31-3.20)			
No. reflections	24325 (2369)			
R_{work}/ R_{free} (%)	19.6 (33.6) /25.2 (38.2)			
No. atoms	8742			
RNA	7586			
Protein	1048			
Ion	86			
Water	22			
Mean *B*-factors (Å^2)	128.0			
RNA	118.7			
Protein	192.7			
Ligand/ion	176.4			
Water	64.2			
R.m.s. deviations				
Bond lengths (Å)	0.001			
Bond angles (°)	0.37			

Supplementary Information

Co-crystal structure of a T-box riboswitch stem I domain in complex with its cognate tRNA

Jinwei Zhang & Adrian R. Ferré-D'Amaré*

National Heart, Lung and Blood Institute

50 South Drive, MSC 8012

Bethesda, MD, 20892-8012, USA

(*) Address correspondence to this author. E: adrian.ferre@nih.gov

T: 301-496-4096, F: 301-451-5459

Supplementary Discussion

Organization of the interdigitated T-loop motif.

The interface with tRNA (layer 1) is formed by C44 (position 3 of T-loop 1), A56 (position -2 of T-loop 2) and G63 (position +1 of T-loop 2). Two base triples (layers 3 and 4) form the core of the domain. In these layers, nucleotides at positions 1 and 5 of the two T-loops close each pentaloop through non-Watson-Crick base pairs (Hoogsteen-Hoogsteen A42•A46 in T-loop 1; WC-Hoogsteen U58•A62 in T-loop 2), while a conserved guanine (G43 or G59) at position 2 of the other T-loop forms a base triple with the 1•5 closing pair using its sugar edge. This exposes the Hoogsteen face of the position 2 guanine to solvent, available for coordination by divalent cations. Substitution of either closing pair with a G•G pair is strongly destabilizing, reducing tRNA binding by ~2 orders of magnitude (A42G/A46G and U58G/A62G, Fig. 2e). Similarly, removal of the sugar edge exocyclic amine by substituting guanines with adenines at position 2, either completely or strongly abrogated tRNA binding (G43A of T-loop 1 and G59A of T-loop 2, respectively, Fig. 2e). Equivalent substitutions of T-loop 1 consistently produce larger tRNA binding defects than those of T-loop 2, presumably reflecting the proximity of T-loop 1 to the tRNA interface. Unlike RNase P[1] and the ribosome[2], the T-box uses a base triple on layer 1 to stack on the tRNA elbow. A Watson-Crick pair (C44•G63) stacks on tG19 while A56 (phylogenetically most commonly a guanine, as in the *B. subtilis glyQS stem I*, Extended Data Fig. 1) stacks on tC56. This arrangement results in a displaced, energetically near-optimal stacking conformation (Fig. 2c) rather than the energetically less favorable "sandwich" arrangement[3,4]. Watson-Crick pairing at the base triple is not obligatory for effective stacking of stem I with the tRNA elbow, as the double substitution C44A/G63A only produced a less than 3-fold effect (Fig. 2e). Reversing the GC pair through a C44G/G63C substitution, however, led to a larger defect (13-fold, Fig. 2e). This could indicate that this double substitution places G44 in unfavorable "sandwich" stacking with tG19, and leave C63 unstacked from tG19 (Fig. 2c). Substituting pyrimidines for either of the two purines of the base triple (G56U or G63C) causes significant defects in tRNA binding whereas a transition mutation (G56A) is well tolerated. These findings are in good agreement with the cocrystal structure and the phylogenetic prevalence of purines at the distal base triple (Fig. 2e, Extended Data Fig. 1).

Supplementary References

1. Reiter, N. J. *et al*. Structure of a bacterial ribonuclease P holoenzyme in complex with tRNA. *Nature* **468**, 784-789 (2010).
2. Korostelev, A., Trakhanov, S., Laurberg, M. & Noller, H. Crystal structure of a 70S ribosome-tRNA complex reveals functional interactions and rearrangements. *Cell* **126**, 1065-1077 (2006).
3. Burley, S. K. & Petsko, G. A. Weakly polar interactions in proteins. *Adv. Prot. Chem.* **39**, 125-192 (1988).
4. Burley, S. K. & Petsko, G. A. Aromatic-aromatic interaction: a mechanism of protein structure stabilization. *Science* **229**, 23-28. (1985).